



**HAL**  
open science

## Genetic diversity and virulence gene profiling of *Vibrio harveyi* in a vibriosis-affected European seabass (*Dicentrarchus labrax*) aquaculture tank

Alix da Fonseca Ferreira, Alice Lehmann, Roxane Roquigny, Thierry Grard,  
Cédric Le Bris

### ► To cite this version:

Alix da Fonseca Ferreira, Alice Lehmann, Roxane Roquigny, Thierry Grard, Cédric Le Bris. Genetic diversity and virulence gene profiling of *Vibrio harveyi* in a vibriosis-affected European seabass (*Dicentrarchus labrax*) aquaculture tank. *Marine Pollution Bulletin*, 2025, 212, pp.117553. 10.2139/ssrn.4956372 . hal-04889440

HAL Id: hal-04889440

<https://ulco.hal.science/hal-04889440v1>

Submitted on 15 Jan 2025

**HAL** is a multi-disciplinary open access archive for the deposit and dissemination of scientific research documents, whether they are published or not. The documents may come from teaching and research institutions in France or abroad, or from public or private research centers.

L'archive ouverte pluridisciplinaire **HAL**, est destinée au dépôt et à la diffusion de documents scientifiques de niveau recherche, publiés ou non, émanant des établissements d'enseignement et de recherche français ou étrangers, des laboratoires publics ou privés.



Distributed under a Creative Commons Attribution 4.0 International License

# 1 Genetic diversity and virulence gene profiling of *Vibrio harveyi* in a 2 vibriosis-affected European seabass (*Dicentrarchus labrax*) aquaculture 3 tank

4 A. Da Fonseca Ferreira, A. Lehmann, T. Grard, R. Roquigny and C. Le Bris

5 Univ. Littoral Côte d'Opale, UMRt 1158 BioEcoAgro, USC ANSES, INRAE, Univ. Artois, Univ. Lille, Univ. Picardie Jules Verne, Univ.  
6 Liège, Junia, F-62200 Boulogne-sur-Mer, France

## 9 Abstract

10 Aquaculture is crucial in meeting global seafood demand; however, intensification often leads to bacterial  
11 diseases that threaten productivity. *Dicentrarchus labrax*, a key species in European aquaculture, is highly  
12 vulnerable to vibriosis, primarily caused by *Vibrio harveyi*. This study investigates genetic profiles associated  
13 with vibriosis by analyzing *V. harveyi* strains from a seabass farm during 2022 vibriosis outbreaks. Sampling  
14 from biofilm and water environments yielded 946 bacterial isolates, of which 56 were identified as *V.*  
15 *harveyi* using MALDI-TOF MS. ERIC-PCR genotyping revealed four distinct profiles. Despite observing  
16 variability in the presence of the 80 tested virulence genes, the overall genetic variation among these profiles  
17 was not pronounced. Notably, no single genotypic profile was linked to vibriosis. These findings suggest that  
18 the presence of virulence genes alone may not predict disease outbreaks, thus highlighting the need for future  
19 research on environmental and transcriptional factors to improve disease control in aquaculture systems.

## 20 1 Introduction

21 Aquaculture is a rapidly expanding industry that plays a crucial role in meeting the global demand for seafood.  
22 The European seabass (*Dicentrarchus labrax*) is among the most economically significant species in European  
23 aquaculture. Its production has experienced substantial growth, reaching 80,786 metric tons and a value of  
24 470 million euros in 2020 in Europe (EUMOFA, 2022). Despite this growth and progress in husbandry  
25 techniques, the European seabass remains highly susceptible to diseases such as vibriosis, caused by bacteria  
26 of the *Vibrio* genus. Vibriosis can lead to significant mortality events, posing a major challenge to the industry,  
27 with symptoms such as ulcers, hemorrhages, and tissue necrosis. Among the Harveyi clade, *Vibrio harveyi* is  
28 particularly problematic in European seabass aquaculture due to its pathogenicity and virulence (Zhang et al.,  
29 2020). A critical early step in studying *V. harveyi* is differentiating it from other species within the clade, as  
30 their genetic similarities make accurate identification difficult. Furthermore, not all *V. harveyi* strains  
31 necessarily provoke vibriosis. Methods like ERIC-PCR (enterobacterial repetitive intergenic consensus-  
32 polymerase chain reaction) have been effectively used to investigate genetic variation among *V. harveyi*  
33 isolates, which can help to explain differences in virulence and pathogenicity (Bai et al., 2020; Xu et al., 2017).  
34 In a pivotal study, Xu et al. (2017) applied ERIC-PCR to *V. harveyi* strains isolated from cultured fish in southern  
35 China, demonstrating its effectiveness in distinguishing between pathogenic and non-pathogenic strains so as  
36 to create genetic fingerprints linked to virulence and identify specific isolates associated with mortality events.

37 Building on these findings, it is essential to further investigate how different genotypic profiles correlate with  
38 variations in virulence. This is particularly important since the pathogenic mechanisms of *V. harveyi* are  
39 complex and not yet fully understood, in part due to the species' high genetic diversity. Thus, it is necessary  
40 to focus on known virulence genes in *V. harveyi*, in the literature and databases, as well as potential virulence  
41 genes in other *Vibrio* species. These bacteria are prone to gene transfer both within and across species, a  
42 phenomenon that is facilitated by their ability to form biofilms (Fu et al., 2022). In aquaculture systems,  
43 bacterial communities exist as biofilms on surfaces and as planktonic bacteria in the water column. The  
44 virulence of these two forms may differ, highlighting the need to study both kinds of isolates in order to  
45 manage disease outbreaks effectively. In this study, we collaborated with a farm that experienced two vibriosis  
46 outbreaks in July and August 2022. It was crucial to analyze bacterial isolates from these episodes to gain  
47 insights into the strains potentially involved. Sampling was conducted to identify the strain(s) responsible.  
48 Initially, *Vibrionaceae* were collected, and bacterial isolates were identified by MALDI-TOF MS and a  
49 combination of the Bruker and Luvibase databases (Mougin et al., 2020). Following identification, ERIC-PCR  
50 was used to type the *V. harveyi* isolates and categorize them into genomic profiles. To provide insights into *V.*  
51 *harveyi* pathogenesis, the presence in isolates of 80 virulence genes potentially implicated in vibriosis was  
52 subsequently investigated. By elucidating the genetic diversity and virulence characteristics of *V. harveyi* in  
53 both biofilms and planktonic phases, the goal was to try to link a genetic profile with vibriosis outbreaks, and  
54 to identify the major virulence genes associated with this profile for future transcriptomic studies. This  
55 approach could be applied to detect the emergence in aquaculture tanks of problematic strains early on,  
56 thereby facilitating the development of targeted antivirulence strategies against these major virulence genes.  
57 Ultimately, this would help advance more sustainable aquaculture practices.

## 58 2 Materials and methods

### 59 2.1 Sample collection and treatment

60 Between May and November 2022, we conducted a sampling campaign at Aquanord-Ictus, an aquaculture  
61 facility in Gravelines (France), along the southwest coast of the North Sea (Da Fonseca Ferreira et al., 2024).  
62 The chosen outdoor aquaculture tank for the study had a volume of approximately 975 cubic meters and  
63 accommodated up to 68,000 sea bass, with an average density of 32 kg per cubic meter. Daily feeding and  
64 oxygenation were maintained to ensure optimal dissolved oxygen levels. During the study period, two  
65 outbreaks of vibriosis attributed to *Vibrio harveyi* were recorded by a veterinary laboratory collaborating  
66 closely with the farm (data not shown). These outbreaks occurred in July and August, necessitating two rounds  
67 of curative oxytetracycline treatment exclusively prescribed by the veterinarian. Sampling followed the  
68 methodology described in Da Fonseca Ferreira et al. (2024). Briefly, biofilm samples were collected using five  
69 cylindrical concrete specimens positioned at three depths (0.3 m, 2.15 m, and 4 m) on different ropes along  
70 the tank walls. Additionally, 15-liter water samples were collected per sampling, with five 1-liter samples taken

71 at each depth using a submersible pump. Sixteen sampling events were conducted, resulting in a total of 240  
72 individual water samples and 240 biofilm samples over the study period. Water samples were filtered through  
73 0.45- $\mu\text{m}$  and 0.22- $\mu\text{m}$  nitrocellulose filters to capture bacteria. Concrete specimens were retrieved, preserved  
74 in sterile water, and swabbed. Samples were stored in Luria-Bertani broth with 20% NaCl and glycerol at -80  
75 °C. Prior to analysis, samples were thawed, vortexed, and centrifuged to obtain cell pellets. A 100- $\mu\text{L}$  aliquot  
76 from each sample was enriched in 1 mL of LBS for 24 hours, followed by inoculation onto thiosulfate-citrate-  
77 bile salts-sucrose (TCBS) agar (Becton Dickinson Difco, Franklin Lakes, NJ, USA) using a 10  $\mu\text{L}$  inoculation loop.  
78 All agar plates were then incubated overnight at 35 °C, which allows growth for many *Vibrio* species (Farmer  
79 III et al., 2015). One colony of each visually different morphotype was randomly selected from each plate and  
80 further individually cultured on marine agar (MA; Condalab, Madrid, Spain) at 35 °C overnight. Pure bacterial  
81 cultures were preserved in LBS broth supplemented with 20% glycerol and stored at -80 °C until identification  
82 through MALDI-TOF MS.

83

## 84 2.2 Bacterial identification using MALDI-TOF MS

85 After thawing, 10  $\mu\text{L}$  of bacterial isolates was cultured and incubated for 24 hours at 35 °C in 2 mL of marine  
86 broth (MB) (Becton Dickinson Difco, Franklin Lakes, NJ, USA) in a 96 deep-well Masterblock (Greiner Bio-One,  
87 Frickenhausen, Germany). The isolates were identified using MALDI-TOF by the EQUIPEX REALCAT platform  
88 (Lille, France). Briefly, the fresh bacterial cultures were centrifuged, and the pellets extracted using 70% formic  
89 acid (Alfa Aesar, Kandel, Germany) and 100% acetonitrile (Biosolve Chimie). Protein extracts were then  
90 deposited in four replicates on a ground steel MTP 384 target plate (Bruker Daltonics, Bremen, Germany)  
91 overlaid with an  $\alpha$ -cyano-4-hydroxycinnamic acid matrix (Sigma-Aldrich, St. Louis, MO, USA), and analyzed  
92 using the Autoflex Speed MALDI-TOF MS (Bruker Daltonics, Bremen, Germany). MALDI-TOF MS profiles were  
93 compared with profiles in the Bruker BioTyper database (version 9.0.0.0) implemented with an in-house *Vibrio*  
94 database known as Luvibase (Mougin et al., 2020). The level of concordance between the experimental  
95 MALDI-TOF MS profiles and the MSPs was quantified using a log score. Specifically, a log score greater than  
96 2.3 indicated a highly probable identification at the species level, while a lower log score ranging from 2.0 to  
97 2.3 indicated a probable identification. Scores within the range of 1.7 to 2.0 suggested a probable identification  
98 at the genus level, while scores below 1.7 indicated a notable absence of substantial similarities between the  
99 MSPs contained in the databases and the unknown sample profile. Identification was considered reliable with  
100 scores of at least 2 for 3 out of 4 deposition replicates.

## 101 2.3 ERIC-PCR and GELJ analysis

102 All the isolates identified as *V. harveyi* by MALDI-TOF-MS were grown overnight at 35 °C on TCBS plates. DNA  
103 was extracted using the DNeasy Blood and Tissue Kit (Qiagen, Hilden, Germany) following the manufacturer's  
104 recommendations. The purity of the DNA was assessed using a NanoDrop 8000 spectrophotometer (Thermo

105 Scientific, Waltham, U.S.), and the concentration of samples was measured with the Qubit™ dsDNA Broad  
106 Range Assay Kit on a Qubit™ 4 fluorometer (Thermo Scientific, Waltham, U.S.). ERIC-PCR was conducted in a  
107 final volume of 25 µL, containing 12.5 µL of Master Mix PCR (2x) (Thermo Fisher Scientific, Waltham, MA, USA),  
108 8 µL of sterile water, 1 µL of each ERIC primer at 10 pmol/µL (ERIC1R: 5'-ATGTAAGCTCTGGGGATTAC-3' and  
109 ERIC2: 5'-AAGTAAGTGAAGTGGGGTGAGCG-3'; TIB MOLBIOL, Syntheselabor GmbH, Germany) (Xu et al., 2017),  
110 and 2.5 µL of extracted DNA (20 ng/µL). The amplification step was performed using a Bio-Rad iCycler (Bio-  
111 Rad, Hercules, CA, USA) with the following cycling conditions: initial denaturation at 95 °C for 7 min, followed  
112 by 35 cycles of denaturation at 90 °C for 30 seconds, annealing at 52 °C for 1 min, then elongation at 65 °C for  
113 8 min. A final elongation step was carried out at 68 °C for 16 min. Subsequently, 10 µL of a mixture of 10 µL of  
114 PCR products and 3 µL of loading buffer (6X) (Lonza, Basel, Switzerland) were loaded onto a 1.5% agarose gel  
115 and stained with ethidium bromide (1% solution) (Fisher BioReagent, Powai, India). Electrophoresis was  
116 performed using a FastGene 100 bp DNA marker (Nippon Genetics, Tokyo, Japan) as a reference. DNA was  
117 migrated on gel at 120 V for 60 min. UV transillumination was used for visualizing results, and images were  
118 captured using an E-Box CX5 TS Edge (Vilber, Marne-la-Vallée, France). Each ERIC-PCR assay was performed in  
119 at least triplicate. The ERIC-PCR fingerprints of amplified DNA fragments, obtained through agarose gel  
120 electrophoresis, were analyzed using GelJ software (version 2.3), designed for constructing phylogenetic trees  
121 from DNA fingerprints. Band positions were normalized using the FastGene 100 bp DNA marker (Nippon  
122 Genetics), with manual correction for accuracy. A dendrogram was generated to represent the genetic  
123 relatedness among *Vibrio harveyi* isolates. The Dice similarity coefficient and UPGMA method were used to  
124 assess and cluster the profiles, resulting in the classification of the *V. harveyi* isolates into four distinct profiles  
125 with an 83% similarity cut-off.

## 126 2.4 Primer design for virulence genes and PCR

### 127 2.4.1 Virulence gene selection and primer design

128 From the sequenced genomes of seven vaccine strains recovered from the aquaculture farm (data neither  
129 shown nor published), a predictive list of virulence genes was established by GenoScreen (Lille, France) for  
130 each isolate. We further analyzed these genomes using VF Analyzer (based on the Virulence Factor Database,  
131 VFDB) to identify virulence genes in each genome (consulted on September 2022). FASTA sequences were  
132 analyzed with VF Analyzer to confirm the consistency of virulence gene identification by GenoScreen. Seventy-  
133 six genes common to at least two vaccine strains were thus selected for primer design. To complement this  
134 list, four genes identified through the literature and not listed among the 76 genes previously mentioned were  
135 included: *V. harveyi* R Toxin (*toxRvh*), *V. harveyi* hemolysin (*vhh*), thermostable direct hemolysin (*tdh*), and a  
136 gene involved in the flagellar system (*flaC*) (Table S1). Virulence gene sequences were retrieved from the  
137 vaccine strains' genomes using the CLC Genomics Workbench (QIAGEN, version 12.0.1). Sequences of the  
138 genes added from the literature were taken from the NCBI with the following accession numbers: DQ503438.1

139 (*toxRvh*), JN033877.1 (*vhh*), NZ\_QOUW02000047.1 (*tdh*) and EU240947.1 (*flaC*). The 80 primer pairs were  
140 designed using Primer3Plus (version 3.2.6), avoiding potential primer dimers or hairpin structures when  
141 possible. If unavoidable, primers with secondary structures having a  $\Delta G$  (Gibbs free energy change) greater  
142 than -3.0 kcal/mol were selected. All primers were validated using the CLC Genomics Workbench with seven  
143 vaccinal genomes and BLAST to ensure specificity to *V. harveyi* and a lack of mutations. All primers had a  
144 melting temperature ( $T_m$ ) around or equal to 60 °C and a GC content close or equal to 55%. Primers were  
145 aligned on the genomes of the vaccine strains to ensure that they were present in a single copy. The primers  
146 (Table S1) were ordered from TIB MOLBIOL (Syntheselabor GmbH).

#### 147 2.4.2 PCR for virulence genes

148 To explore a potential correlation between the occurrence of virulence genes in *V. harveyi* and their ERIC  
149 profiles while trying to limit the number of isolates to study, two isolates maximum per profile were selected  
150 for complementary analysis, except for profile 2 which included only one isolate, resulting in a total of seven  
151 isolates being profiled. The 80 virulence genes were screened using PCR across these seven *V. harveyi* selected  
152 isolates. A no-template control was included and each virulence gene PCR was conducted at least in duplicate.  
153 To evaluate the PCR functionality of virulence genes, the 80 primer pairs were tested on the isolate they were  
154 designed from. Each primer pair underwent triplicate testing alongside a no-template control to verify its  
155 functionality. Each PCR reaction was conducted in a 25  $\mu\text{L}$  volume, consisting of 12.5  $\mu\text{L}$  of 2x Master Mix PCR  
156 (Thermo Fisher Scientific), 9  $\mu\text{L}$  of sterile water, 0.5  $\mu\text{L}$  of each primer at 10 pmol/ $\mu\text{L}$ , and 2.5  $\mu\text{L}$  of extracted  
157 DNA (20 ng/ $\mu\text{L}$ ). The reactions were carried out using a Bio-Rad iCycler (Bio-Rad) with a standardized protocol  
158 for all genes: initial denaturation at 95 °C for 2 min, followed by 35 cycles of denaturation at 95 °C for 30 s,  
159 annealing at 55 °C for 30 s, and elongation at 72 °C for 45 s, concluding with a final extension step at 72 °C for  
160 10 min. Subsequently, 10  $\mu\text{L}$  of a mixture of 10  $\mu\text{L}$  PCR products and 3  $\mu\text{L}$  loading buffer (6X) (Lonza) were  
161 deposited on 1.5% agarose gels stained with ethidium bromide (1% solution) (Fisher BioReagent).  
162 Electrophoresis was performed in the same way as above with ERIC-PCR.

## 163 3 Results

### 164 3.1 Identification of isolates

165 A total of 946 bacterial isolates—383 from biofilm and 563 from water—were collected using TCBS agar (Figure  
166 1). They were all identified with a MALDI-TOF analysis using Bruker and Luvibase databases, and identification  
167 was reliable, with scores of at least two for three out of four replicates. Among the biofilm samples, 309  
168 isolates were identified as *Vibrio alginolyticus*, while 482 isolates were found in the water samples. *Vibrio*  
169 *harveyi* was also identified in 31 biofilm isolates and 25 water isolates. Other notable species included *Vibrio*  
170 *parahaemolyticus*, with 29 isolates in total (11 in biofilm samples and 18 in water samples), *Vibrio rotiferianus*  
171 with seven isolates (four in biofilm samples and three in water samples), and *Vibrio owensii* with five isolates  
172 (three in biofilm samples and two in water samples). Additionally, certain species were unique to the water

173 samples: *Shewanella algae* with seven isolates, *Vibrio mytili* with two isolates, *Vibrio diazotrophicus* with one  
174 isolate, and *Shewanella indica* with one isolate.

### 175 3.2 *V. harveyi* ERIC-PCR fingerprinting

176 The 56 isolates of *Vibrio harveyi* were thoroughly examined using ERIC-PCR profiling, revealing significant  
177 genetic diversity among the isolates. The similarity indices of the dendrogram constructed from the ERIC-PCR  
178 profiles ranged from 75% to 100%, indicating a broad spectrum of genetic diversity (Figure S1). Using an 83%  
179 cut-off, the isolates were classified into four distinct ERIC-PCR genotypes. This classification facilitated the  
180 analysis of genomic profile distribution according to the sampling month, type of sample (water or biofilm),  
181 and sampling depth (top, middle, bottom) (Figure 2). The analysis of the distribution of *V. harveyi* profiles  
182 across the water column and months revealed a consistent presence of the species from May to November,  
183 with varying ERIC profile distributions (Figure 2). Profile 1 contained four isolates, primarily collected from the  
184 bottom of the tank in November. Profile 2 was represented by a single isolate collected in July from the middle  
185 of the tank, coinciding with the first observed outbreak of vibriosis. Profile 3 comprised 41 isolates and was  
186 consistently found throughout the sampling period across all depths (top, middle, bottom) and in both water  
187 and biofilm samples. Profile 4 contained 10 isolates, predominantly collected from biofilms (eight out of 10).  
188 This profile emerged in July, persisted throughout August during the second vibriosis outbreak, reappeared in  
189 October, and disappeared in November.

### 190 3.3 Genotyping of virulence genes in the profiles

191 After successfully validating the designed primers and confirming their amplicon sizes, we investigated the  
192 occurrence of virulence genes among two isolates per distinct *V. harveyi* genomic profile (Figure 3). The  
193 isolates representing each profile were as follows: profile 1 included isolates B15B3-3 and E15B5-1; profile 2  
194 consisted of isolate E4M2-2 (only isolate); profile 3 included isolates E1M3-3 and B4M5-1; and profile 4  
195 included isolates B10B5-2 and B13M1-1 (internal nomenclature). Among the seven isolates studied, a majority  
196 harbored most of the genes examined, but several significant differences were noted. Profile 1 contained all  
197 the screened genes associated with chemotaxis signaling, flagellar assembly and function, pilus assembly,  
198 secretion system, hemolysin, iron acquisition, exopolysaccharide (EPS) biosynthesis, capsule, and toxin  
199 regulation. These isolates shared nearly identical sets of genes crucial for environmental adaptation and host  
200 interaction, with minor variations observed in E15B5-1, which harbored multiple bands for genes *flaB*, *motX*,  
201 *motY*, *mshG*, and *mshL*. Profile 2, characterized by isolate E4M2-2, lacked the *mshA* gene but had all the other  
202 analyzed genes. Profile 3 contained all the genes except for the virulence-associated *vcrV* in E1M3-3 and lacked  
203 *mshA* in B4M5-1, which is crucial for pilus biosynthesis. Profile 4, comprising isolates B10B5-2 and B13M1-1  
204 isolated from biofilms, showcased distinct genetic profiles with specific gene deficiencies. B10B5-2 lacked  
205 flagellar genes *flgD*, *flgF*, *flgK*, *flgL*, *flhF*, *fliK*, *fliR*, *flrB*, pilus gene *pilB*, virulence factors *vcrV*, *vhh*, *vctA*, and EPS  
206 biosynthesis gene *epsF*. In contrast, B13M1-1 lacked flagellar genes *flgD*, *flgE*, *flgG*, *flgH*, *flgM*, *flhA*, pilus

207 assembly gene *mshA*, and EPS biosynthesis gene *epsF*, and possessed multiple bands for *mshG*, *mshL*, and *vcrD*  
208 genes, along with a shorter variant of *vscC*. This indicates that isolates from the same profile do not  
209 systematically share exactly the same genes.

## 210 4 Discussion

211 The mere presence of *Vibrio harveyi* in aquaculture environments does not necessarily lead to vibriosis  
212 outbreaks (Mougin et al., 2021), as the development of the disease is influenced by a complex interplay of  
213 abiotic and biotic factors (Montánchez and Kaberdin, 2020). Although *V. harveyi* is a well-established primary  
214 causative agent of vibriosis, its virulence potential is also shaped by what virulence genes the isolates in the  
215 tank harbor. The overarching goal of our study was to identify the genetic profile(s) linked to vibriosis and  
216 associated mortality. Our study specifically aimed to investigate the genetic diversity of *V. harveyi* in both  
217 water and biofilms, characterize its virulence gene profiles, and analyze its relative temporal and spatial  
218 distribution on a sea bass farm in northern France. The ultimate goal is to develop a method for detecting  
219 problematic bacteria in the tanks before they cause disease outbreaks. Sampling was conducted from May to  
220 November 2022. During this period, the farm experienced two significant vibriosis outbreaks attributed to *V.*  
221 *harveyi*, one in July and another one in August. The unpredictable nature of the *Vibrio harveyi*-associated  
222 vibriosis episodes in the farm further highlights the need to explore the genetic diversity of the strains and  
223 attempt to understand which ones are responsible for these outbreaks. In analyzing the bacterial populations  
224 within the tank, we used TCBS selective media to isolate a total of 946 visually distinct colonies from both  
225 biofilm (383 isolates) and water samples (563 isolates), with a focus on *Vibrionaceae* but also including some  
226 other species. MALDI-TOF identification revealed a variety of *Vibrio* species, with *Vibrio alginolyticus* being the  
227 most prevalent. This species accounted for 309 isolates from biofilm and 482 from water samples. *Vibrio*  
228 *alginolyticus* thrives in warm coastal waters and is often associated with severe infections and high mortality  
229 in species like sea bass, making it a significant concern in aquaculture (Abdel-Aziz et al., 2013). *Vibrio*  
230 *alginolyticus* is not the sole problematic species in our case, as *V. harveyi*, the causative agent of two outbreaks  
231 during the campaign, was also present, though in smaller numbers (31 biofilm isolates and 25 water isolates).  
232 Furthermore, the bacterial isolates were selected visually, which may have led to more *V. alginolyticus*  
233 colonies being isolated due to greater morphological variation, while *V. harveyi* might have had more visually  
234 similar isolates. In a previous study conducted at the same farm in 2018, when no vibriosis outbreaks occurred  
235 and sampling was limited to the surface water of a smaller tank (75 m<sup>3</sup>, 1.3 meters deep), *V. harveyi* and *V.*  
236 *alginolyticus* were present in approximately equal amounts, along with *Photobacterium damsela* subsp.  
237 *damsela* regardless of the sampling site and sample type (Mougin et al., 2021). This earlier finding  
238 underscores the need to consider both biotic and abiotic factors to better understand vibriosis development.  
239 Under favorable environmental conditions, co-infection with *V. harveyi* can significantly enhance the  
240 pathogenic effects of other species. For instance, co-infection between *V. harveyi* and *V. alginolyticus* has been

241 shown to worsen vibriosis symptoms in hybrid groupers (*Epinephelus polyphekadion* × *E. fuscoguttatus*)  
242 (Mohamad et al., 2019). Studies also indicate that *V. harveyi* and *V. alginolyticus* were also found with *V.*  
243 *parahaemolyticus* in superficial lesions among Asian seabass (*Lates calcarifer*) (Liu et al., 2016). Several  
244 bacteria other than *Vibrio* species were identified in our samples, including *Shewanella algae* and *Shewanella*  
245 *indica*, which were unique to biofilm samples. *Shewanella* species have been implicated in mixed infections  
246 with *Vibrio* species across various teleost fish species, further underscoring the increased threat of mixed  
247 infections in aquaculture (Sony et al., 2021). In light of the challenges in examining all the concurrent species  
248 during *Vibrio* outbreaks, it is essential to concentrate on *V. harveyi* to determine whether some genetic profiles  
249 are specific to vibriosis episodes. To classify and group genetically similar *V. harveyi* isolates present during  
250 the campaign, we employed ERIC-PCR, which generates detailed 'fingerprint-like' profiles for each isolate. This  
251 technique is cost-effective and well-suited for analyzing genetic diversity in *Vibrio* species, including *V. harveyi*  
252 (Bai et al., 2020; Kahla-Nakbi et al., 2006; Su and Chen, 2020; Xu et al., 2017; Yang et al., 2021). In our study,  
253 ERIC-PCR revealed distinct banding patterns among the isolates, with amplicon numbers ranging from 4 to 11  
254 and fragment sizes from 100 bp to over 4 kb, underscoring the substantial genetic diversity within the *V.*  
255 *harveyi* population. The 56 isolates were classified into four ERIC-PCR genotypes (Figure S1) using an 83%  
256 similarity cut-off. However, this classification does not produce homogeneous groups in terms of number of  
257 isolates, leading to uneven distribution of the isolates across the profiles. For each profile, isolates were  
258 selected to represent variation in one parameter: type (biofilm or water), depth (top, middle, bottom). To  
259 evaluate if any profile exhibited increased pathogenic potential, we screened 80 genes associated with  
260 virulence in the seven isolates representing the diversity of genetic profiles (Figure 3). Within these profiles,  
261 we observed differences in the occurrence of genes. In profile 1, one isolate out of two, originating from the  
262 bottom of the water column, showed multiple amplicons for motility and pilus assembly genes. This  
263 phenomenon may be attributed to the presence of multiple gene variants, where imperfect hybridization  
264 during amplification forms heteroduplexes that migrate more slowly during electrophoresis than perfectly  
265 matched pairs, resulting in multiple bands (Moreno et al., 2002). Profile 2 included a single isolate, exhibiting  
266 all the studied genes except *mshA*. The absence of *mshA* reduces the ability to form biofilm, crucial for  
267 environmental persistence, and increases resistance to VGJ4 phage infection (Ledón et al., 2012; Sinha-Ray  
268 and Ali, 2017). Therefore, this isolate is particularly intriguing and merits further study due to its possession of  
269 several virulence genes, potential filamentous bacteriophage resistance, and its presence during the initial  
270 vibriosis outbreak month. Compared with other profiles with multiple isolates, it would be valuable to obtain  
271 additional isolates with this profile to confirm the presence or absence of these genes. Profile 3 was the most  
272 sampled, potentially because it encompasses the majority of isolates—41 in total—collected from various  
273 depths (top, middle, and bottom) as well as from both water and biofilm samples. The large number of isolates  
274 in this profile may explain the genetic differences observed between the two isolates representing it.

275 Therefore, further investigation of additional isolates using ERIC-PCR would be beneficial, as analyzing only  
276 two isolates may not fully capture the genetic diversity within this profile. Profile 4 included 10 isolates,  
277 predominantly collected from biofilm samples. Both of the profile 4 isolates selected exhibited distinct genetic  
278 adaptations compared with the other three profiles, highlighting specialized strategies for biofilm survival.  
279 Both isolates displayed deficiencies in flagellar genes, potentially reducing motility, favoring attachment within  
280 biofilms, and decreasing virulence (McGee et al., 1996). Like profile 3 isolates, profile 4 isolates showed  
281 absences or multiple bands for flagellar, pilus assembly and secretion system genes, though they were not the  
282 same in the two isolates. They also exhibited deficiencies in *epsF*, suggesting reduced EPS biosynthesis (Kong  
283 et al., 2022). One isolate in profile 4 also lacked *vhh* and *vctA*, genes associated with hemolysis and iron  
284 acquisition, respectively, which could potentially impair their pathogenicity. The other isolate had a truncated  
285 amplicon for the *vscC* gene, possibly due to a deletion that could impair its function and render *V. harveyi* less  
286 virulent and more susceptible to abiotic factors (Mao et al., 2021; Zhang et al., 2021). Given the observed  
287 diversity both among and within profiles, it would be useful to investigate whether there is a temporal pattern  
288 or succession of profiles that could explain the development of vibriosis. Analyzing the temporal distribution  
289 of *V. harveyi* profiles across the water column revealed that the species was consistently present from May to  
290 November, with variations in isolate and ERIC profile distributions (Figure 2). This finding is supported by qPCR  
291 quantification, which confirmed the continuous presence of *V. harveyi* throughout the sampling campaign (Da  
292 Fonseca Ferreira et al., 2024). Profile 1 was primarily collected in November. Profile 2, collected in July,  
293 coincided with the first vibriosis outbreak. Profile 3 was consistently found throughout the sampling period.  
294 Profile 4, predominantly collected from biofilms, emerged in July, persisted through the second outbreak in  
295 August, reappeared in October, and disappeared in November. However, when examining the virulence genes,  
296 it is not clear whether a specific profile is responsible for the vibriosis outbreaks, as nearly all the profiles  
297 contain most of the targeted genes. The only exception is profile 4, which diverges from the others by lacking  
298 some key genes. Like Xu et al. (2017), our study identified genetic diversity among *V. harveyi* isolates, but a  
299 major difference is that they first conducted pathogenicity challenges, grouping all pathogenic strains into the  
300 same profile. Within this profile, not all strains possessed the virulence genes they investigated. In contrast,  
301 our study focused on environmental isolates and aimed to detect genetic diversity linked to the timing and  
302 occurrence of vibriosis outbreaks, resulting in the identification of four distinct profiles, most of which  
303 contained virulence genes. However, given the large number of virulence genes involved in various  
304 mechanisms, it is challenging to determine whether a specific profile is responsible for the development of  
305 vibriosis. While ERIC-PCR proved to be a rapid, efficient, and cost-effective method for distinguishing isolates,  
306 it did not pinpoint a specific profile linked to vibriosis. Our findings suggest that merely detecting virulence  
307 genes may not fully capture the pathogenic potential. However, this work is crucial for understanding genetic  
308 diversity and guiding future research, which should focus on exploring these virulence factors under varying

309 environmental and host-specific conditions to mimic natural vibriosis outbreaks. This includes conducting  
310 bacterial challenge studies to test the isolates, to identify which ones are pathogenic and which ones are not.  
311 Subsequently, it is essential to consider the expression of the studied virulence genes in those that cause  
312 disease, as recommended in studies of *Vibrio* fish infections (Hernández-Cabanyero et al., 2022; Wang et al.,  
313 2022). By unraveling the transcriptional dynamics of these virulence genes, future studies could advance our  
314 understanding of how *V. harveyi* induces vibriosis in *D. labrax*. Such investigations into genetic diversity,  
315 virulence genes, and pathogenic mechanisms are pivotal for predicting disease outbreaks and developing  
316 targeted strategies for disease prevention and control in aquaculture settings.

## 317 5 Conclusion

318 This study highlights the complex dynamics of *Vibrio harveyi* in aquaculture, focusing on its genetic diversity  
319 and virulence potential. Our findings reveal two key aspects of *V. harveyi*'s role in vibriosis outbreaks on a sea  
320 bass farm. First, ERIC-PCR revealed genetic diversity among *V. harveyi* isolates, identifying distinct genotypic  
321 profiles. This variability in gene occurrence may influence the pathogen's behavior and adaptability, indicating  
322 that *V. harveyi* isolates are not uniform. Such diversity could enhance the pathogen's persistence and its  
323 interactions with the environment and host. Second, the analysis of virulence genes across profiles revealed  
324 that while many isolates possess genes linked to pathogenicity—such as those for biofilm formation, motility,  
325 and EPS biosynthesis—no single profile was clearly and specifically associated with vibriosis outbreaks. This  
326 suggests that virulence potential is influenced more by the interplay between genetic diversity and  
327 environmental factors than by the presence of individual genes alone. These findings emphasize the critical  
328 need to consider both biotic and abiotic environmental factors along with strain-specific virulence profiles  
329 when evaluating the risk and management of vibriosis in aquaculture systems (Da Fonseca Ferreira et al., 2024;  
330 Mougin et al., 2021; Roquigny et al., 2021). Future research should explore how genetic diversity impacts  
331 virulence under various environmental and host conditions, and investigate the transcriptional responses of  
332 virulence genes. Given the complexity of the tripartite interaction, one goal is to understand the influence and  
333 relationship between each part to better anticipate vibriosis outbreaks. These studies are crucial for enhancing  
334 predictions and management of disease outbreaks in aquaculture systems, as global warming is likely to alter  
335 the distribution and abundance of *Vibrio* species, and increase the frequency and severity of such events (Ma  
336 et al., 2023; Trinanes and Martinez-Urtaza, 2021).

## 337 6 Acknowledgements

338 The authors would like to thank Aquanord-Ichthus, and especially Guillaume Tielie, Annabelle Duhamel, and  
339 Céline Doyen. We are also grateful to the REALCAT platform funded by a French government grant  
340 administered by the French National Research Agency (ANR) as part of the “Investments for the Future”  
341 program (ANR-11-EQPX-0037). We would also like to thank Enola Blaise, Lorédane Clause and Margaux Lay

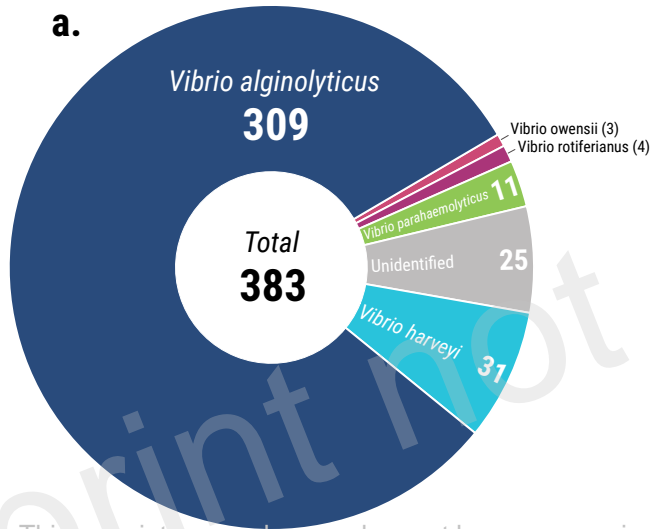
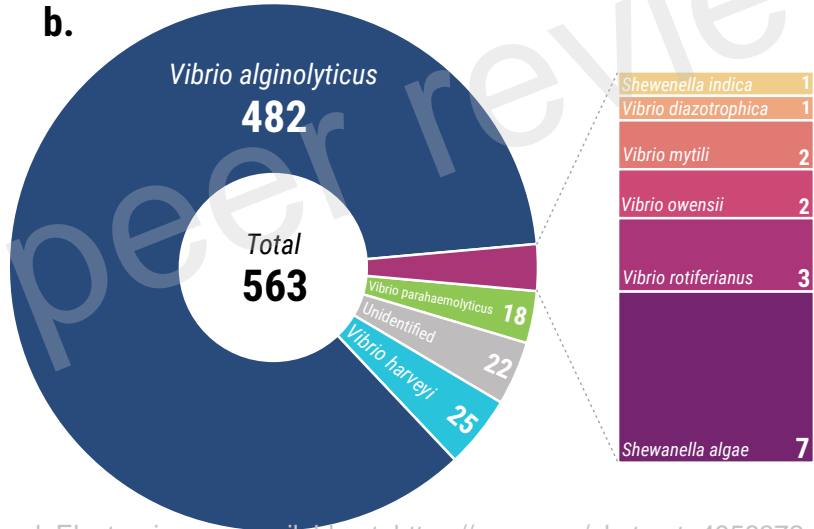
342 for technical support, and Dr Christophe FLAHAUT for his expertise in mass spectrometry. Alix Da Fonseca  
343 Ferreira would like to thank the PMCO council and Hauts-de-France regional council for their financial support  
344 of her PhD studies. This work was funded by the French government, Ifremer and the Hauts-de-France region  
345 in the framework of the CPER 2021–2027 IDEAL project and the IFSEA Graduate School (stemming from the  
346 National Research Agency under the “Investments for the Future” program, ANR-21- EXES-00 11).

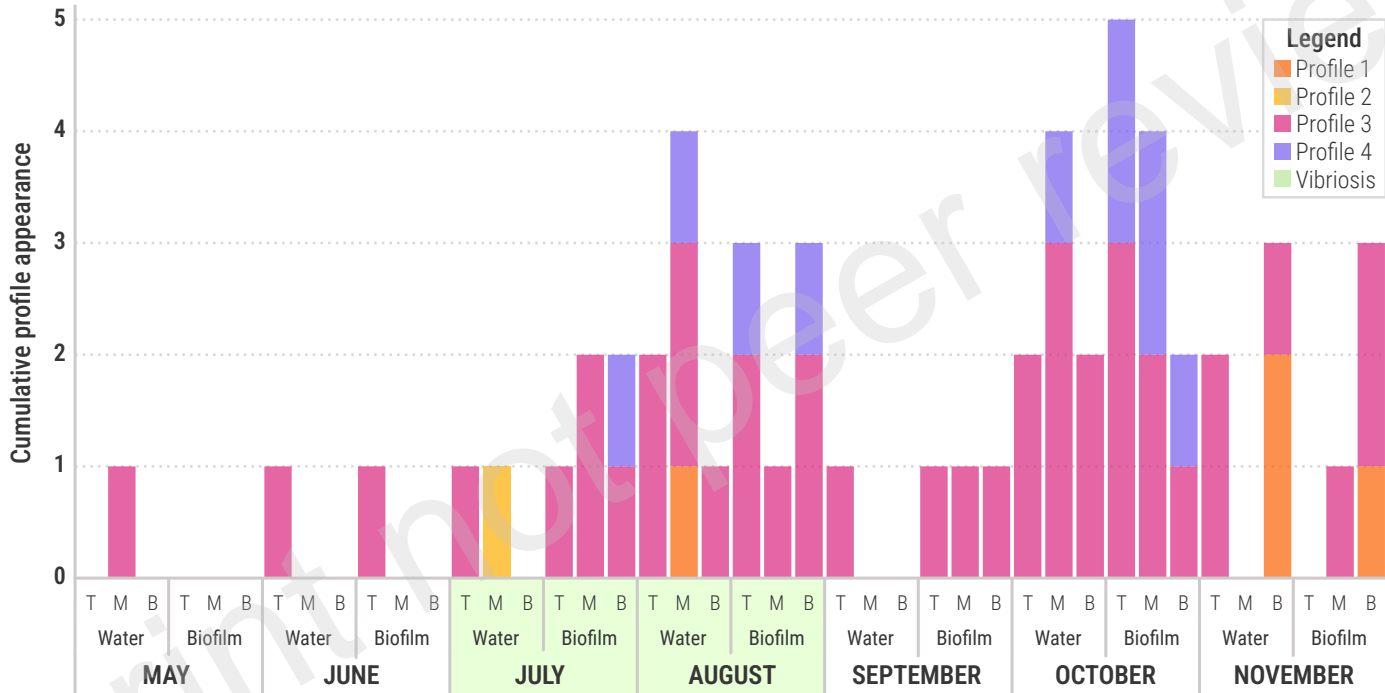
## 347 7 Bibliography

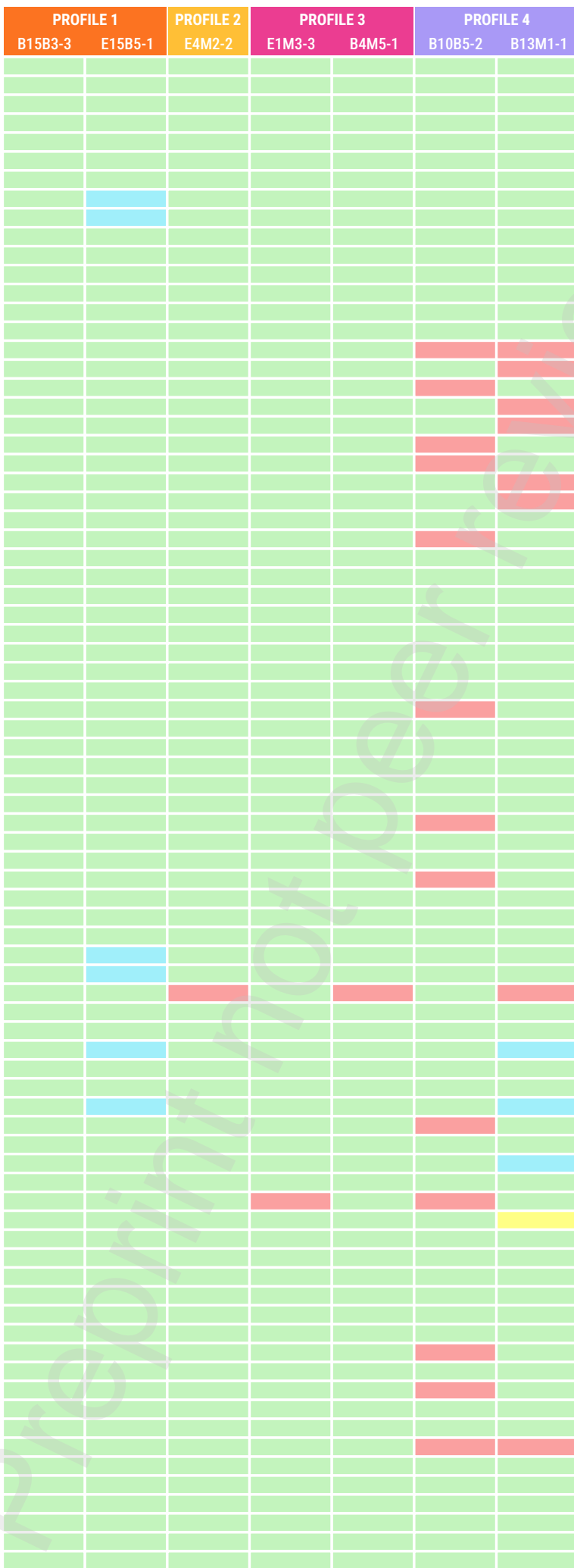
- 348 Abdel-Aziz, M., Eissa, A.E., Hanna, M., Okada, M.A., 2013. Identifying some pathogenic  
349 *Vibrio/Photobacterium* species during mass mortalities of cultured Gilthead seabream (*Sparus*  
350 *aurata*) and European seabass (*Dicentrarchus labrax*) from some Egyptian coastal provinces. *Int. J.*  
351 *Vet. Sci.* 1, 87–95. <https://doi.org/10.1016/j.ijvsm.2013.10.004>
- 352 Bai, J.-Y., Long, H., Cui, J., Zhang, X., Cai, X.-N., Xie, Z.-Y., 2020. Characterization of a pathogenic *Vibrio harveyi*  
353 strain from diseased *Epinephelus coioides* and evaluation of different methods to control its  
354 infection. *Aquaculture* 526, 735371. <https://doi.org/10.1016/j.aquaculture.2020.735371>
- 355 Da Fonseca Ferreira, A., Roquigny, R., Grard, T., Le Bris, C., 2024. Temporal and spatial dynamics of *Vibrio*  
356 *harveyi*: An environmental parameter correlation investigation in a 4-metre-deep *Dicentrarchus*  
357 *labrax* aquaculture tank. *Microorganisms* 12, 1104.  
358 <https://doi.org/10.3390/microorganisms12061104>
- 359 EUMOFA, 2022. The EU fish market: 2022 edition. Publications Office, LU.
- 360 Farmer III, J. j., Michael Janda, J., Brenner, F.W., Cameron, D.N., Birkhead, K.M., 2015. *Vibrio*, in: *Bergey’s*  
361 *Manual of Systematics of Archaea and Bacteria*. John Wiley & Sons, Ltd, pp. 1–79.  
362 <https://doi.org/10.1002/9781118960608.gbm01078>
- 363 Fu, S., Wang, Q., Wang, R., Zhang, Y., Lan, R., He, F., Yang, Q., 2022. Horizontal transfer of antibiotic  
364 resistance genes within the bacterial communities in aquacultural environment. *Sci. Total Environ.*  
365 820, 153286. <https://doi.org/10.1016/j.scitotenv.2022.153286>
- 366 Hernández-Cabanyero, C., Sanjuán, E., Reyes-López, F.E., Vallejos-Vidal, E., Tort, L., Amaro, C., 2022. A  
367 transcriptomic study reveals that fish vibriosis due to the zoonotic pathogen *Vibrio vulnificus* is an  
368 acute inflammatory disease in which erythrocytes may play an important role. *Front. Microbiol.* 13.  
369 <https://doi.org/10.3389/fmicb.2022.852677>
- 370 Kahla-Nakbi, A.B., Chaieb, K., Besbes, A., Zmantar, T., Bakhrouf, A., 2006. Virulence and enterobacterial  
371 repetitive intergenic consensus PCR of *Vibrio alginolyticus* strains isolated from Tunisian cultured  
372 gilthead sea bream and sea bass outbreaks. *Vet. Microbiol.* 117, 321–327.  
373 <https://doi.org/10.1016/j.vetmic.2006.06.012>
- 374 Kong, L., Xiong, Z., Song, X., Xia, Y., Ai, L., 2022. CRISPR/dCas9-based metabolic pathway engineering for the  
375 systematic optimization of exopolysaccharide biosynthesis in *Streptococcus thermophilus*. *J. Dairy*  
376 *Sci.* 105, 6499–6512. <https://doi.org/10.3168/jds.2021-21409>
- 377 Ledón, T., Ferrán, B., Pérez, C., Suzarte, E., Vichi, J., Marrero, K., Oliva, R., Fando, R., 2012. TLP01, an *mshA*  
378 mutant of *Vibrio cholerae* O139 as vaccine candidate against cholera. *Microbes Infect.* 14, 968–978.  
379 <https://doi.org/10.1016/j.micinf.2012.04.004>
- 380 Liu, L., Ge, M., Zheng, X., Tao, Z., Zhou, S., Wang, G., 2016. Investigation of *Vibrio alginolyticus*, *V. harveyi*,  
381 and *V. parahaemolyticus* in large yellow croaker, *Pseudosciaena crocea* (Richardson) reared in  
382 Xiangshan Bay, China. *Aquaculture Reports* 3, 220–224. <https://doi.org/10.1016/j.aqrep.2016.04.004>
- 383 Ma, J.-Y., Zhu, X.-K., Hu, R.-G., Qi, Z.-Z., Sun, W.-C., Hao, Z.-P., Cong, W., Kang, Y.-H., 2023. A systematic  
384 review, meta-analysis and meta-regression of the global prevalence of foodborne *Vibrio* spp.  
385 infection in fishes: A persistent public health concern. *Mar. Pollut. Bull.* 187, 114521.  
386 <https://doi.org/10.1016/j.marpolbul.2022.114521>
- 387 Mao, F., Liu, K., Wong, N.-K., Zhang, X., Yi, W., Xiang, Z., Xiao, S., Yu, Z., Zhang, Y., 2021. Virulence of *Vibrio*  
388 *alginolyticus* accentuates apoptosis and immune rigor in the Oyster *Crassostrea hongkongensis*.  
389 *Front. Immunol.* 12. <https://doi.org/10.3389/fimmu.2021.746017>

- 390 McGee, K., Hörstedt, P., Milton, D.L., 1996. Identification and characterization of additional flagellin genes  
391 from *Vibrio anguillarum*. J. Bacteriol. 178, 5188–5198. [https://doi.org/10.1128/jb.178.17.5188-](https://doi.org/10.1128/jb.178.17.5188-5198.1996)  
392 5198.1996
- 393 Mohamad, N., Mohd Roseli, F.A., Azmai, M.N.A., Saad, M.Z., Md Yasin, I.S., Zulkipli, N.A., Nasruddin, N.S.,  
394 2019. Natural Concurrent infection of *Vibrio harveyi* and *V. alginolyticus* in cultured hybrid groupers  
395 in Malaysia. J. Aquat. Anim. Health 31, 88–96. <https://doi.org/10.1002/aah.10055>
- 396 Montánchez, I., Kaberdin, V.R., 2020. *Vibrio harveyi*: A brief survey of general characteristics and recent  
397 epidemiological traits associated with climate change. Mar. Environ. Res. 154, 104850.  
398 <https://doi.org/10.1016/j.marenvres.2019.104850>
- 399 Moreno, C., Romero, J., Espejo, R.T., 2002. Polymorphism in repeated 16S rRNA genes is a common property  
400 of type strains and environmental isolates of the genus *Vibrio*. Microbiology 148, 1233–1239.  
401 <https://doi.org/10.1099/00221287-148-4-1233>
- 402 Mougín, J., Flahaut, C., Roquigny, R., Bonnin-Jusserand, M., Grard, T., Le Bris, C., 2020. Rapid identification of  
403 *Vibrio* species of the Harveyi clade using MALDI-TOF MS profiling with main spectral profile database  
404 implemented with an in-house database: Luvibase. Front. microbiol. 11, 586536.  
405 <https://doi.org/10.3389/fmicb.2020.586536>
- 406 Mougín, J., Roquigny, R., Flahaut, C., Bonnin-Jusserand, M., Grard, T., Le Bris, C., 2021. Abundance and  
407 spatial patterns over time of *Vibrionaceae* and *Vibrio harveyi* in water and biofilm from a seabass  
408 aquaculture facility. Aquaculture 542, 736862. <https://doi.org/10.1016/j.aquaculture.2021.736862>
- 409 Roquigny, R., Mougín, J., Le Bris, C., Bonnin-Jusserand, M., Doyen, P., Grard, T., 2021. Characterization of the  
410 marine aquaculture microbiome: a seasonal survey in a seabass farm. Aquaculture 531, 735987.  
411 <https://doi.org/10.1016/j.aquaculture.2020.735987>
- 412 Sinha-Ray, S., Ali, A., 2017. Mutation in *flrA* and *mshA* genes of *Vibrio cholerae* inversely involved in *vps*-  
413 independent biofilm driving bacterium toward nutrients in lake water. Front. Microbiol. 8, 1770.  
414 <https://doi.org/10.3389/fmicb.2017.01770>
- 415 Sony, M., Sumithra, T.G., Anusree, V.N., Amala, P.V., Reshma, K.J., Alex, S., Sanil, N.K., 2021. Antimicrobial  
416 resistance and virulence characteristics of *Vibrio vulnificus*, *Vibrio parahaemolyticus* and *Vibrio*  
417 *harveyi* from natural disease outbreaks of marine/estuarine fishes. Aquaculture 539.  
418 <https://doi.org/10.1016/j.aquaculture.2021.736608>
- 419 Su, C., Chen, L., 2020. Virulence, resistance, and genetic diversity of *Vibrio parahaemolyticus* recovered from  
420 commonly consumed aquatic products in Shanghai, China. Mar. Pollut. Bull. 160, 111554.  
421 <https://doi.org/10.1016/j.marpolbul.2020.111554>
- 422 Trinanes, J., Martínez-Urtaza, J., 2021. Future scenarios of risk of *Vibrio* infections in a warming planet: a  
423 global mapping study. Lancet Planet Health 5, e426–e435. [https://doi.org/10.1016/S2542-](https://doi.org/10.1016/S2542-5196(21)00169-8)  
424 5196(21)00169-8
- 425 Wang, J., Chen, Z., Xu, W., Li, Y., Lu, S., Wang, L., Song, Y., Wang, N., Gong, Z., Yang, Q., Chen, S., 2022.  
426 Transcriptomic analysis reveals the gene expression profiles in the spleen of spotted knifejaw  
427 (*Oplegnathus punctatus*) infected by *Vibrio harveyi*. Dev. Comp. Immunol. 133, 104432.  
428 <https://doi.org/10.1016/j.dci.2022.104432>
- 429 Xu, X., Liu, K., Wang, S., Guo, W., Xie, Z., Zhou, Y., 2017. Identification of pathogenicity, investigation of  
430 virulent gene distribution and development of a virulent strain-specific detection PCR method for  
431 *Vibrio harveyi* isolated from Hainan Province and Guangdong Province, China. Aquaculture 468, 226–  
432 234. <https://doi.org/10.1016/j.aquaculture.2016.10.015>
- 433 Yang, A., Li, W., Tao, Z., Ye, H., Xu, Z., Li, Y., Gao, Y., Yan, X., 2021. *Vibrio harveyi* isolated from marine  
434 aquaculture species in eastern China and virulence to the large yellow croaker (*Larimichthys crocea*).  
435 J. Appl. Microbiol. 131, 1710–1721. <https://doi.org/10.1111/jam.15070>
- 436 Zhang, X.H., He, X., Austin, B., 2020. *Vibrio harveyi*: a serious pathogen of fish and invertebrates in  
437 mariculture. Mar. Life. Sci. Technol. 1–15. <https://doi.org/10.1007/s42995-020-00037-z>
- 438 Zhang, Y., Deng, Y., Feng, J., Guo, Z., Chen, H., Wang, B., Hu, J., Lin, Z., Su, Y., 2021. Functional  
439 characterization of VscCD, an important component of the type III secretion system of *Vibrio*  
440 *harveyi*. Microb. Pathog. 157, 104965. <https://doi.org/10.1016/j.micpath.2021.104965>

Preprint not peer reviewed

**a.****b.**





Chemotaxis

Flagellar assembly & function

Pilus assembly

Secretion system

Hemolysin

Iron acquisition

Exopolysaccharide biosynthesis

Capsule

Toxin regulation

Gene occurrence : Present Absent Multiple bands Smaller band

## Figures captions

Figure 1: Donut plots of species found in the bacterial isolates sampled in an aquaculture tank, grown on TCBS agar and identified using MALDI-TOF mass spectrometry. Plot a. shows bacteria collected in the biofilm samples, and b. shows bacteria collected in the water samples.

Figure 2: Distribution of the ERIC profiles of the 56 *Vibrio harveyi* isolates and their cumulative appearance over months, sample type, and depth (T: top; M: middle; B: bottom) collected during sampling in the aquaculture tanks. The months with recorded vibriosis outbreaks are highlighted in green.

Figure 3: Heatmap of the potential virulence genes studied across the four identified ERIC profiles and their functions. Green: the gene is present with an expected amplicon size; red: the gene is absent; blue: the expected amplicon is present but with multiple bands; yellow: the amplicon is smaller than expected.